Mach Wave Emission from Supersonic Jets

S.P. Parthasarathy* and P.F. Massier†
Jet Propulsion Laboratory, Pasadena, Calif.

An experimental investigation has been conducted on supersonic jets at a Mach number of 1.43 over a temperature range from about 420 K to 1370 K (300°F to 2000°F) in which it was found that the noise in the far field was dominated by eddy Mach waves. It is shown both from experimental and theoretical considerations that the strength of the Mach waves is determined by the product of the mean shear and the density fluctuations of the jet. Thus, the source of sound arises from the mixing of hot and cold streams as well as from those compressions and expansions that are intuitively associated with sound generation. For the temperature range investigated, the Mach waves were emitted at angles between 37 and 59 deg with respect to the jet axis with the smaller angle occurring at the lower temperature, which is also at the lower jet velocity. These values represent those in the region of the jet where the Mach angle was constant, that is, beginning at the nozzle exit and extending downstream to a distance ranging from 5 to 12 jet diameters, depending on temperature.

Nomenclature

a_0 = ambient speed of sound
C = correlation coefficient
D = nozzle exit diameter
M = Mach number referred to ambient speed of sound
M_j = Mach number of the jet referred to the speed of sound at the jet temperature
p = static pressure
r = radial coordinate
S = distance along boom
t = time
U = mean velocity at any point in the shear layer
U_j = velocity of the jet at the nozzle exit
u = instantaneous velocity
V = wave speed
X = position vector of microphone outside the jet
x = Cartesian coordinate outside the jet
Y = position vector inside the jet
y = Cartesian coordinate inside the jet
Z = defined by Eq. (10)
γ = specific heat ratio
θ = angle between X-Y and the x axis
ξ = eddy coordinate
ρ = density
ρ_j = density inside the jet
τ = time scale of fluctuations
ϕ = angle in Fig. 2
( ) = function of
[ ]{ } = products
⟨ ⟩ = time average

Subscripts

1,2 = microphones
1,2,3 = three components of a vector
0 = ambient condition
P,Q = microphones
i,j,k,ℓ = tensor indices
r = direction of sound radiation

Superscript

′ = fluctuation

Introduction

A REVIEW of the studies that led to the conclusion that Mach waves dominate the radiation field for supersonic turbulent flow is given by Ffowcs-Williams and Maidanik.[1] In that paper the authors developed a theory for estimating the Mach wave radiation from a supersonic turbulent shear flow based on a description of the density fluctuations within the flow. Experimental results on jet flows were needed to substantiate the conclusions drawn from their theory.

More recently, a comparatively detailed experimental investigation was conducted by Parthasarathy et al.[2] with a supersonic jet in which density fluctuations in the flow were obtained using a crossed-beam laser-Schlieren method. The Mach number at the nozzle exit was 1.43, and the stagnation temperature was 1090 K (1500°F). Using the experimental information of the density fluctuations and of the mean shear obtained from probe measurements, the autocorrelation of the radiated noise was calculated utilizing a modified version of the theory of Ffowcs-Williams and Maidanik.[1] For this procedure it was not necessary to make use of any adjustable constants. The noise calculated in this manner agreed within about 5 dB of the overall sound pressure level obtained from the signals detected by microphones located outside the jet.

In the present investigation results were obtained for eddy Mach waves emitted from jets that ranged in stagnation temperature between about 420 K and 1370 K (300°F and 2000°F). The purpose was to verify that density fluctuations resulting from the mixing of hot and cold streams over a broad range of temperature did contribute to the sound generation and that the dominant sound emission mechanism was by eddy Mach waves. The Mach number at the nozzle exit was 1.43. In this case, experimental values of the density fluctuations throughout the jet flow were not determined. Consequently, the theory of Ffowcs-Williams and Maidanik[1] was modified so that the predicted sound pressure level could be calculated using the density and the mean velocity of the flow at the nozzle exit. This modification was accomplished by dimensional analysis of the relevant equations to derive the proper scaling relations. One of these scaling relations pertains to the sound pressure level in terms of the source, that is, the product of the density fluctuations and the mean shear. The other scaling relation pertains to the time scale of the autocorrelation in terms of the Mach number and the dimensions of the jet.

Theoretical Analysis

The basic equation for the description of Mach wave emission from supersonic flows is given by Ffowcs-Williams and Maidanik.[1] In this equation, the pressure fluctuation p' in the sound field outside the jet is given in terms of the variables inside the flow; namely, the density fluctuation $\partial\rho/\partial t$, the mean shear $\partial U_r/\partial y_r$, and also the velocity fluctuation u_r'.

Presented as Paper 76-505 at the 3rd AIAA Aero-Acoustics Conference, Palo Alto, Calif., July 20-23, 1976; submitted Aug. 18, 1976; revision received May 2, 1977.
Index categories: Aeroacoustics; Supersonic and Hypersonic Flow.
*Member of Technical Staff. Member AIAA.
†Group Supervisor. Associate Fellow AIAA.

A simplification of the exact equation, in which only the term amplified by the mean shear is retained, may be expressed as

$$p'(X,t) = -\frac{1}{4\pi}\int_{\text{vol}} \left\{\frac{\partial\rho}{\partial t}\frac{\partial U_i}{\partial y_j}\right\}\left(Y, t-\frac{|X-Y|}{a_0}\right) \times \frac{[x_i-y_i][x_j-y_j]}{|X-Y|^3}\,dY \tag{1}$$

The assumptions involved in this simplification as stated in Ref. 2 are as follows: 1) the mean velocity gradient is much larger than the fluctuating velocity gradient, and thus $\partial^2\rho u_r'/\partial y_r\partial t$ is negligible; 2) the direction of observation is nearly the same as the direction of Mach wave emission; hence the component of eddy convection velocity U_r is nearly equal to a_0. Thus, the source term $[U_r-a_0]\partial^2\rho/\partial y_r\partial t$ vanishes.

It is of significance to note that the source term in Eq. (1) is expressed in terms of the fluctuating density $\partial\rho/\partial t$ inside the flow; hence the product of this fluctuating density and the mean shear is the basic source of sound. Equation (1) applies to hot as well as to cold jets. Thus, in addition to the mean shear, a contribution to the source of sound arises from the mixing of hot and cold streams as well as from those compressions and expansions that are intuitively associated with sound generation.

In the Mach wave direction, the sound pressure fluctuation is related to the density fluctuation and mean shear in a simple way as shown in Eq. (1). The source term is a simplification of the acoustic stress tensor. Generally, linear terms in fluctuations are not regarded as source terms and are expressed as part of the unknowns in the left-hand side; but from an experimental point of view, an equation can be split in any convenient way and one part of the equation may be regarded as the source for the other. This point of view is more or less forced by nature in the case of high Mach number turbulence because the stress tensor includes sound terms and cannot be estimated separately until the sound radiation problem is solved.

A few remarks on the amplifying role of mean shear on the strength of Mach waves are in order. A volume of fluid (which will be referred to as an eddy) moving supersonically with respect to the ambient fluid outside will generate Mach waves, which are conical fronts attached to this moving volume. The waves are confined to the region occupied by the two cones emanating from the front and from the back of this volume. Mean shear will deform the volume so that it becomes more like a disk. Correspondingly, the extent of the pressure pulse generated by the disk is increased. The magnitude of the pressure rise depends on the angle that the disk makss with respect to the direction of motion, but the pressure rise is unaffected by the shear deformation. A succession of pulses produced by many of such volumes (or eddies) moving in sequence results in a random sound pressure in the radiated field. The mean shear then increases the mean square pressure by increasing the time duration of the pulses. Thus, the mean shear causes the eddies to grow in size. In an axisymmetric jet, if these volume elements that produce the Mach waves are large ringlike structures, the same argument is valid, the only difference being that the Mach wave field would be coherent in the circumferential direction.

In Eq. (1), of the nine mean velocity gradients, only $\partial U_1/\partial y_2$ is significant, because for a jet the other components are small in comparison. Therefore, using only the term with $i=1$ and $j=2$, Eq. (1) becomes

$$p'(X,t) = -\frac{1}{4\pi}\int\left[\frac{\partial\rho}{\partial t}\frac{\partial U_1}{\partial y_2}\right]\left(Y, t-\frac{|X-Y|}{a_0}\right) \times \frac{\sin\theta\cos\theta}{|X-Y|}\,dY \tag{2}$$

The angle θ is the angle between $X-Y$ and the x_1 axis.

To make use of Eq. (2) for predicting the sound pressure level based on some of the experimental results, simplification is necessary. This can be accomplished by a dimensional analysis. The resulting equation will be in a form that includes readily obtainable values of the density and of the mean velocity at the nozzle exit, and geometrical parameters that govern the generation of Mach waves. Equation (2) is not restricted to the far field because, for Mach waves, there is no difference between the near and far field, and measurements may be made anywhere in the radiated sound field outside the jet flow.

Equation (2) first is written in the following form in which $\langle p'^2\rangle$ is expressed in source and geometric terms with two integrations, dY and $d\xi$, over the volume of the jet and over the volume of the eddy, respectively:

$$\langle p'^2\rangle \sim \int\int\left\langle\left[\frac{\partial\rho}{\partial t}\frac{\partial U_1}{\partial y_2}\right]^2\right\rangle\frac{\sin^2\theta\cos^2\theta}{|X-Y|^2}\,dY\,d\xi \tag{3}$$

The contribution to the sound source from $[\partial\rho/\partial t]^2$ arises from both mixing and from compressibility effects. If it is assumed that these two effects add as mean squares,

$$\left[\frac{\partial\rho}{\partial t}\right]^2 \sim \frac{[M_j^2\rho_j]^2+[\rho_0-\rho_j]^2}{\tau^2} \tag{4}$$

Next, the density ρ, is nondimensionalized by ρ_0 and the time scale τ, by D/a_0. Equation (4) then may be expressed as

$$\left[\frac{\partial\rho}{\partial t}\right]^2 \sim \frac{[M_j^2(\rho_j/\rho_0)]^2+[(\rho_0-\rho_j)/\rho_0]^2}{[\tau a_0/D]^2} \tag{5}$$

In a linearly growing shear layer, which is the case for a jet, the square of the mean shear can be approximated as

$$\left[\frac{\partial U_1}{\partial y_2}\right]^2 \sim \left[\frac{U_j/a_0}{y_1/D}\right]^2 \tag{6}$$

For Mach waves, θ is the Mach angle as shown in Fig. 1. With appropriate instrumentation the Mach angle can be found directly from experimental data. In addition, from Fig. 1 the distance $|X-Y|$ can be obtained from measurements of the microphone locations relative to the jet axis. In nondimensional form the inverse square law may be expressed in terms of $D^2/|X-Y|^2$.

The integration over the eddy consists of two parts: the first part $a_0\tau$, which is the distance traversed by the eddy in the time scale τ, and the second part which is represented by the cross-sectional area of the eddy normal to the direction of Mach wave propagation. If the eddies are spherical, all cross sections are equal. If, however, they are elongated in the y_1 direction (elliptical), it can be shown that the cross section normal to the wave propagation direction is larger than the vertical cross section by the factor $1/\cos\theta$.

It is assumed here that the eddies are elongated in the y_1 direction, therefore, the factor $1/\cos\theta$, is introduced. The volume of the eddy therefore is given by

$$[a_0\tau/D]\,[y_1^2/D^2\cos\theta]$$

where the eddy area proportional to y_1^2 is used in nondimensional form.

In the next integration, which is over the jet volume, the assumption is made that the source is concentrated in a thin annular cylindrical volume so that the part due to a change of y_2 in $2\pi y_2 dy_2 dy_1$ is not significant. This means that y_2 is replaced by a fixed quantity equal to the jet radius $D/2$. In fact, the integration then is over the variable y_1.

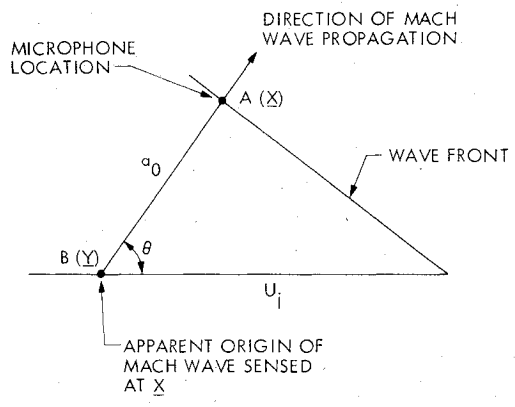

Fig. 1 Diagram of Mach wave propagation. Underlined terms indicate vector.

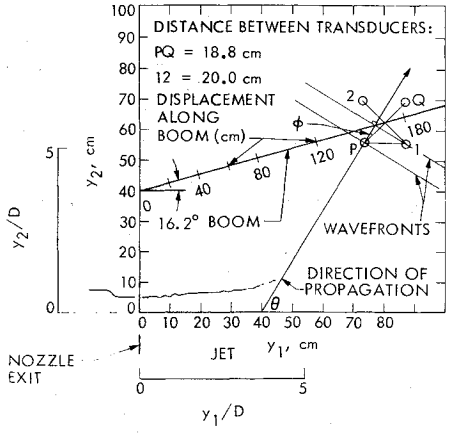

Fig. 2 Instrumentation arrangement.

Because of the linear growth of the shear layer,

$$\int \frac{2\pi y_2 \mathrm{d}y_2}{D^2} \sim \frac{y_1}{D} \tag{7}$$

then

$$\langle p_1'^2 \rangle \sim \int \frac{[M_j^2(\rho_j/\rho_0)]^2 + [(\rho_0-\rho_j)/\rho_0]^2}{[a_0\tau/D]} \left[\frac{U_j}{a_0}\right]^2 \times \frac{D^2 \sin^2\theta \cos\theta}{|X-Y|^2} \left[\frac{y_1}{D}\right] \frac{\mathrm{d}y_1}{D} \tag{8}$$

In Eq. (8) $y_1 \sim \tau$, and therefore $\mathrm{d}y_1$ is the length along y_1 that contributes to Mach wave radiation. In the experiments this radiated noise was sensed by the microphones as shown in Fig. 1. The evaluation of $\mathrm{d}y_1$ in nondimensional form is y_1/D, and the resulting expression after substitution is

$$\langle p_1'^2 \rangle \sim \frac{\{[M_j^2(\rho_j/\rho_0)]^2 + [(\rho_0-\rho_j)/\rho_0]^2\}}{[a_0\tau/D]} \left[\frac{U_j}{a_0}\right]^2 \times \frac{D^2 \sin^2\theta \cos\theta}{|X-Y|^2} \left[\frac{y_1}{D}\right]^2 \tag{9}$$

The sound pressure level (SPL) in dB can be obtained by taking the log of both sides of Eq. (9). Thus,

$$\mathrm{SPL} = 10\log\left\{\left[M_j^2\frac{\rho_j}{\rho_0}\right]^2 + \left[\frac{\rho_0-\rho_j}{\rho_0}\right]^2\right\} + 20\log\left[\frac{U_j}{a_0}\right] - 10\log\left[\frac{a_0\tau}{D}\right] - 20\log\frac{|X-Y|}{D} + 20\log\left[\frac{y_1}{D}\right] + 10\log\cos\theta + 20\log\sin\theta \equiv Z \tag{10}$$

All of the terms on the right side of Eq. (10) were evaluated in the experiments as was the sound pressure level. The results of the experiments are discussed later.

Measurement Techniques and Method of Data Analysis

The sound radiation field was probed with four transducers located at the vertices of a rhombus as shown in Fig. 2. This array was traversed near the jet along a boom set at an angle with respect to the jet axis. P and Q were Kistler transducers and 1 and 2 were ¼-in. B&K microphones. The distance between P and Q was 18.8 cm, whereas the distance between 1 and 2 was 20.0 cm.

The acoustic wave front and the direction of propagation, which is normal to the acoustic wave front, are shown in Figs. 3 and 4. A straight line, drawn between transducers P and Q formed a small angle ϕ with respect to the normal of the wave front as shown in Fig. 2. The signals from the pairs P and Q were cross correlated to obtain the time delays τ_{PQ}, at which the curve produced a maximum. This time is the time of travel of the wave that moves along the ray shown inclined to PQ at an angle ϕ. Signals from 1 and 2 were processed similarly. A line drawn between 1 and 2 formed the same angle ϕ with respect to the wave front. From the configuration of the setup, it can be shown that

$$V\tau_{12}/D_{12} = \sin\phi \tag{11}$$

$$V\tau_{PQ}/D_{PQ} = \cos\phi \tag{12}$$

Therefore,

$$\tan\phi = \frac{\tau_{12}}{\tau_{PQ}} \cdot \frac{D_{PQ}}{D_{12}} = \frac{\tau_{12}}{\tau_{PQ}} \cdot \left[\frac{18.8}{20}\right] \tag{13}$$

and

$$V = 1\Big/\sqrt{\left(\frac{\tau_{12}}{D_{12}}\right)^2 + \left(\frac{\tau_{PQ}}{D_{PQ}}\right)^2} \tag{14}$$

The wavespeed V and the direction ϕ of the wave travel were obtained from the preceding equations. In all of the data to be presented here, V was found to be constant at the ambient speed of sound, equal to 355 m/sec.

Discussion of Results

In Figs. 3 and 4, data on wave direction are shown for the two stagnation temperatures 422 and 1227 K. Experimental data were however, obtained at eight stagnation temperatures: 422, 533, 672, 811, 950, 1089, 1227, and 1366 K. The jet was correctly expanded at a Mach number of 1.43 at the nozzle exit. In these figures, the direction of the sound wave is indicated by an arrow and its length is proportional to the correlation coefficient determined from the signals detected by microphones P and Q. It was found that the Mach waves are emitted at steeper angles to the jet axis as temperature increases. This is a consequence of the high velocity of the jet at the higher temperatures. In Fig. 3 an additional sound radiation is shown that propagates upstream and appears to have its source in the region located 11-14 diam downstream of the nozzle. These waves also exhibit the general wide-band nature of jet noise and may result from large sound sources that occur in the transonic portion of the jet. The properties of these waves, however, need more scrutiny and will not be discussed here. Only those Mach waves that arise from apparent centers beyond 30 cm ($y_1/D = 2.78$) downstream will be discussed in detail.

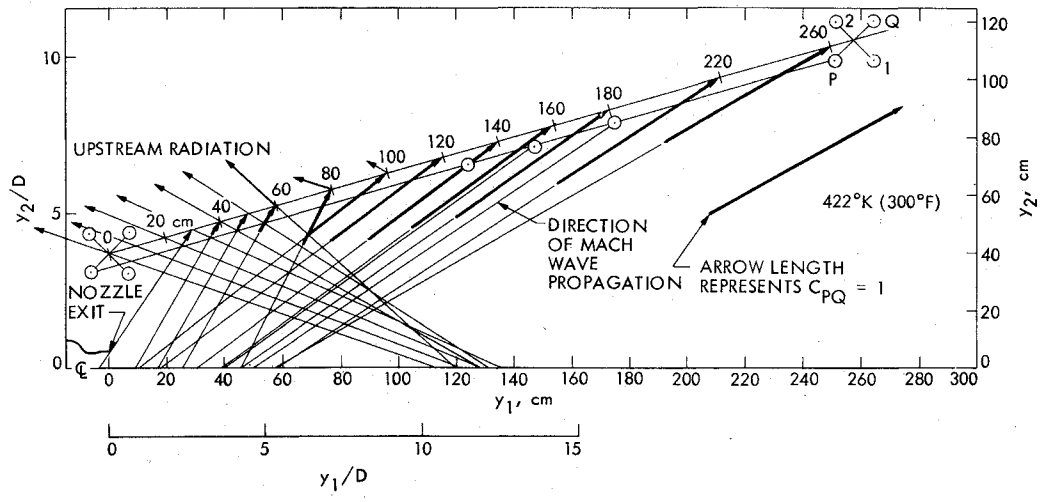

Fig. 3 Mach wave field for a jet temperature of 422 K.

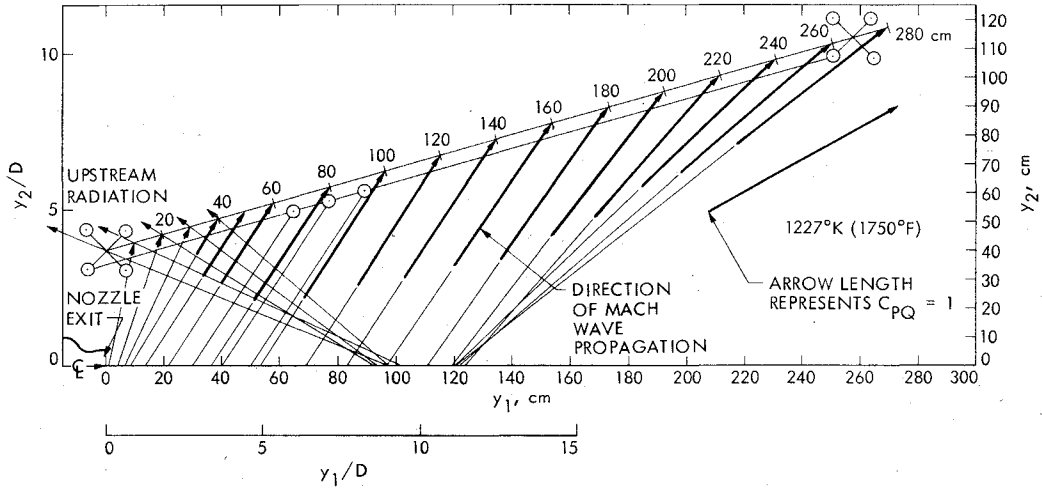

Fig. 4 Mach wave field for a jet temperature of 1227 K.

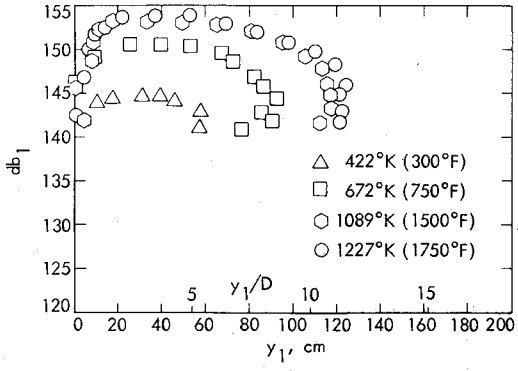

Fig. 5 Intensity of Mach waves at various temperatures vs apparent origin on the jet axis.

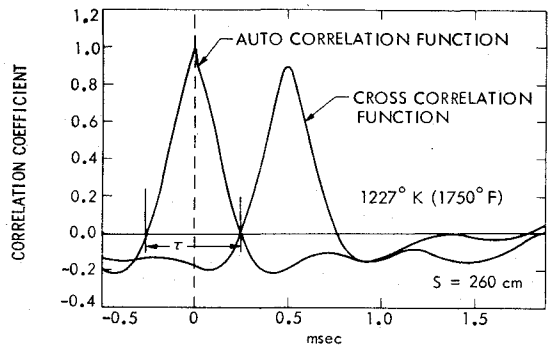

Fig. 6 Typical auto- and cross-correlation coefficients of the Mach wave field sensed by the pair of transducers P and Q.

In Fig. 5 the sound pressure levels for microphone No. 1 are shown plotted as a function of the location of the virtual origin of the Mach waves. Similar results, not shown, were obtained for the other microphones. The levels at lower temperatures are lower, cover a smaller region of the jet, gradually increase in level, and cover larger extents as temperature increases. This is consistent with the fact that, with supersonic jets for which the exit velocities are larger (even though the Mach number may be the same), the supersonic velocity region extends over a larger axial distance. At any given jet temperature the sound pressure levels are approximately constant in the region of Mach wave generation.

The time scale of the autocorrelation function of the sound pressure at transducer P is defined as the time interval between the first zero crossings on either side of the symmetrical function (refer to Fig. 6). This full width is shown plotted as a function of the apparent origin of Mach waves in Figs. 7a-c. For clarity the mean lines through the data points are shown in Fig. 7c. The time scale is proportional to y_1 in the region where the Mach waves are nearly parallel to each other. This occurs from 5 to 10 diam beyond the jet exit location. At large values of y_1 the Mach angle decreases, and, as a consequence, the relationship deviates from a linear one.

The theoretical result is confined to the linear region shown in Fig. 7 because, in the dimensional analysis, linearity has

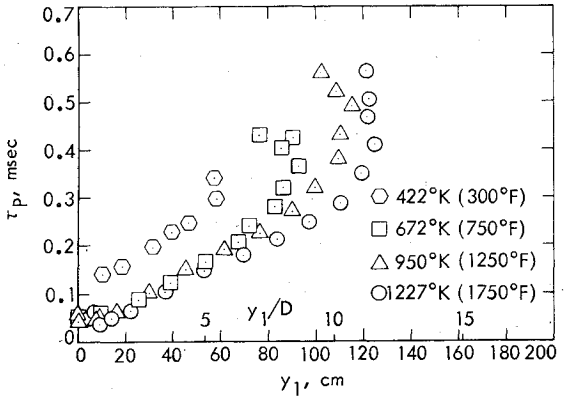

Fig. 7a Growth of the time scale τ_p vs axial distance y_1 at various temperatures.

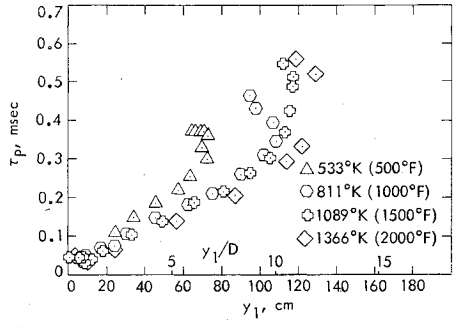

Fig. 7b Growth of time scale τ_p vs axial distance y_1 at various temperatures.

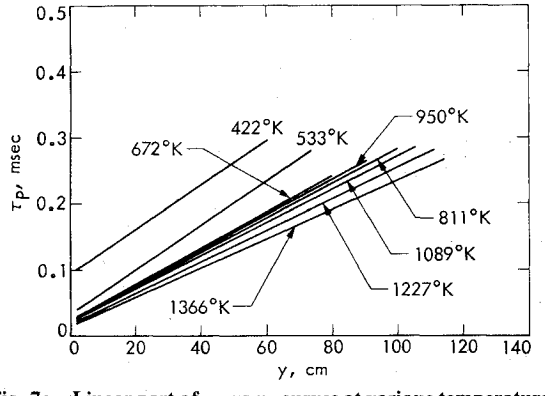

Fig. 7c Linear part of τ_p vs y_1 curves at various temperatures.

been assumed in the integration to produce the similarity relation given by Eq. (10). At a fixed y_1/D, the time scale τ_P decreases with increased flow speed, that is, as the temperature is increased. The nondimensional slope $a_0\ \mathrm{d}\tau_P/\mathrm{d}y_1$ of the straight lines in Fig. 7c vary directly as the reciprocal of the acoustic Mach number U_j/a_0 as shown in Fig. 8.

In the theoretical analysis the density fluctuation in the flow was taken as the sum of the mean squares of the fluctuations caused by the compressibility of the flow and by the fluctuations caused by mixing of the hot and cold streams. By use of a one-dimensional flow approximation the compressibility portion gives the following result:

$$\frac{\mathrm{d}\rho}{\rho} = -M^2\frac{\mathrm{d}u}{u} \tag{15}$$

or

$$\rho' \sim \rho_j M_j^2 [\text{turbulent intensity}] \tag{16}$$

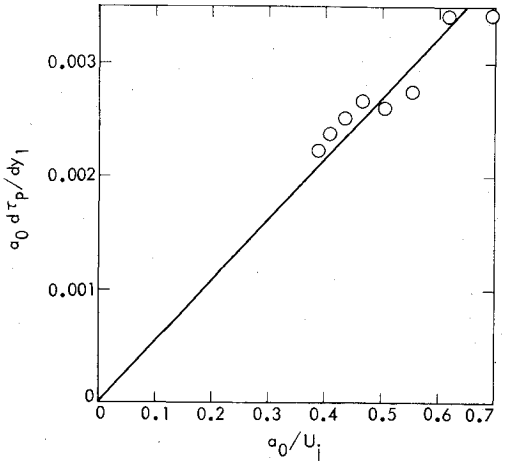

Fig. 8 Nondimensional slope of the Mach wave time scale vs the Mach number of the jet referred to the ambient speed of sound.

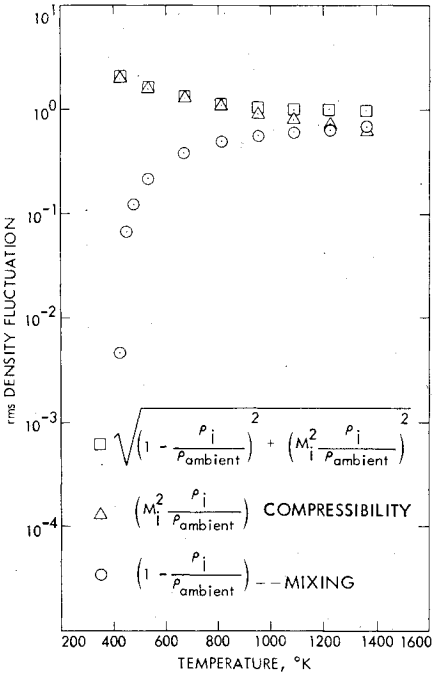

Fig. 9 Combination of the rms density fluctuations from the two components associated with compressibility and mixing of hot and cold streams.

The mixing component results in

$$\rho' \sim [\rho_0 - \rho_j]\,[\text{turbulent intensity}]$$

In nondimensional form the fluctuations resulting from the two causes are $\rho_j M_j^2/\rho_0$ and $(1-\rho_j/\rho_0)$, respectively. In Fig. 9, the two effects are shown separately, together with the root mean square of the combined effect. At temperatures less than about 800 K, the density fluctuation is caused almost entirely by the compressibility, whereas, at a temperature of 1300 K the contributions of compressibility and of mixing are about equal. The total mean square density fluctuation, however, decreases as temperature increases.

In Fig. 10, the sound pressure level as determined by transducer P is plotted as a function of Z. The quantity Z contains many terms, including flow fluctuations and configuration terms as defined by Eq. (10). Data from the locations 30, 40, and 50 cm ($y_1/D = 2.8$, 3.7, and 4.6) downstream of the nozzle exit are shown for various temperatures. The slope of this line should be 45 deg using the

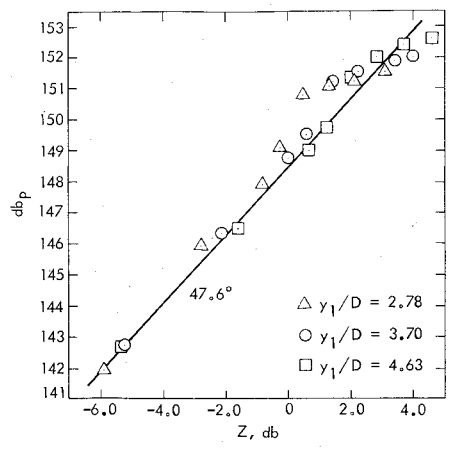

Fig. 10 Intensity of sound at transducer P vs parameter Z containing data at various temperatures.

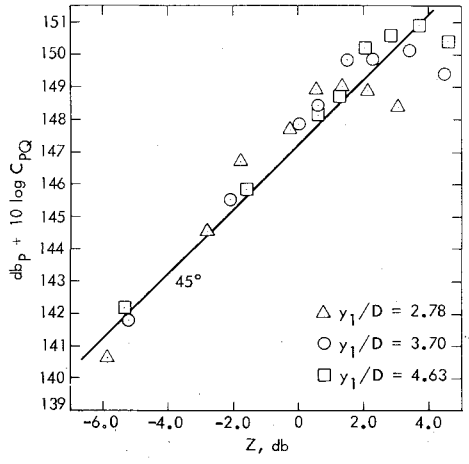

Fig. 11 Intensity of Mach wave radiation at P sensed by the pair of transducers P and Q vs parameter Z containing data at various temperatures.

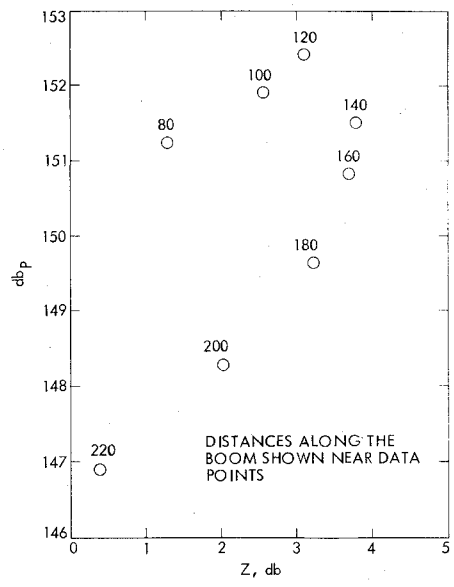

Fig. 12 Intensity of sound at transducer P vs Z for a fixed stagnation temperature of 1089 K.

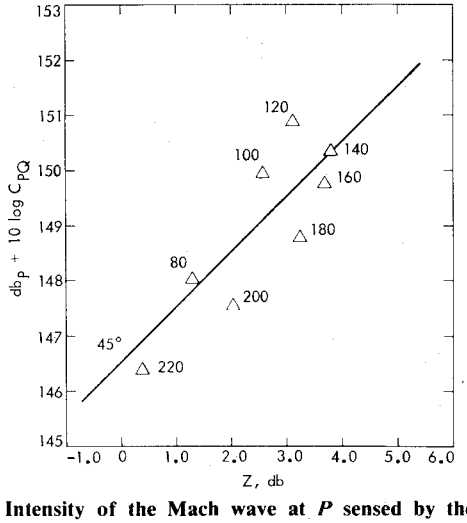

Fig. 13 Intensity of the Mach wave at P sensed by the pair of transducers P and Q vs Z for a fixed stagnation temperature of 1089 K.

prediction of Eq. (10). It is apparent in Fig. 10 that the slope of the straight line is somewhat larger, that is, 47.6 deg. If, however, instead of plotting the measured sound pressure level at P, only the correlated part sensed by the pair of transducers P and Q is plotted vs Z, i.e., $\mathrm{SPL}_P + 10 \log C_{PQ}$ vs Z, the slope agrees with the prediction of Eq. (10) as indicated by a 45-deg slope shown in Fig. 11. This shows that at positions near the nozzle exit, the portion of the sound radiation caused by Mach waves that is sensed by P and Q together correlates with the density fluctuations as expected; however, the total noise sensed by P or Q, which contains radiation in addition to Mach wave emission, does not. Consequently, part of the radiated noise must be emitted by some mechanism other than Mach waves. This portion must be the upstream radiation indicated in Figs. 3 and 4, which appears to originate in the transonic part of the jet flow. The ranges of the magnitudes of C_{PQ} are shown in Table 1. In the regions near the nozzle exit, about half of the noise is emitted as Mach waves, and farther downstream almost all of the noise radiation is transmitted in the form of Mach waves.

Table 1 Results of Mach wave emission from supersonic jets over a jet temperature range for $M_j = 1.43$

Temperature at nozzle exit, K(°F)	Region of Mach wave emission, y_1/D	Mach wave angle with respect to jet axis, θ, deg	Region in which Mach wave angle is constant, y_1/D	Range of C_{12}	Range of C_{PQ}
422 (300)	1.0-5.4	37.0	1.0-4.3	0.13-0.72	0.48-0.90
533 (500)	2.2-6.7	41.0	2.2-5.9	0.26-0.74	0.69-0.94
672 (750)	1.8-8.5	46.5	1.8-7.6	0.21-0.74	0.58-0.91
811 (1000)	2.2-10.0	49.1	2.2-9.4	0.26-0.73	0.66-0.92
950 (1250)	2.6-10.6	53.3	2.6-9.3	0.27-0.77	0.64-0.92
1089 (1500)	2.8-10.8	55.0	2.6-9.7	0.28-0.72	0.64-0.92
1227 (1750)	2.8-11.4	57.0	2.8-10.3	0.27-0.70	0.64-0.90
1366 (2000)	2.8-11.9	59.0	2.8-10.6	0.27-0.71	0.63-0.91

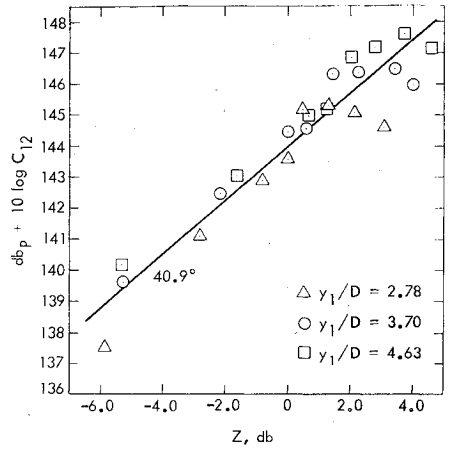

Fig. 14 Intensity of sound at P sensed by the pair of microphones 1 and 2 vs the parameter Z containing data at various temperatures.

To show the dependence of the Mach wave sound pressure levels on parameters other than the density fluctuations, plots of the data at a fixed temperature of 1090 K (1500°F) taken at various positions along the boom are shown in Figs. 12 and 13. In Fig. 12, there is large scatter, and the correction by adding 10 log C_{PQ} to dB_P reduces the scatter. Moreover, the slope is now close to the predicted 45-deg slope.

Microphones 1 and 2 shown in Fig. 3 are oriented such that a Mach wave front passes over them almost simultaneously. The magnitude of the correlation coefficient C_{12} is generally less than C_{PQ} as shown in Table 1. The correlation between transducers set a fixed distance apart is expected to depend on the size of the eddies, which cause the Mach wave radiation, because small eddies radiating at higher frequencies are coherent over a smaller length of the Mach wavefront. This effect is seen in the reduced correlations near the nozzle exit; whereas C_{12} is larger and ≈ 1 farther downstream. Thus, C_{12} is not a proper measure of the strength of Mach waves and the quantity $dB_P + 10 \log C_{12}$ should not correlate with the density fluctuations. Figure 14 shows that this is indeed the case because the slope of $dB_P + 10 \log C_{12}$ vs Z is 40.9 deg.

Conclusions

1) Dimensional analysis of Mach wave generation in terms of density fluctuations and mean shear has been verified experiments covering a range of jet temperatures between 420 and 1370K (300 and 2000°F). The Mach number of the correctly expanded supersonic jet was 1.43 at the nozzle exit.

2) The density fluctuation expressed as the sum of mean squares of the contributions brought about by compressibility and by mixing of the hot and cold streams is consistent with the theory. At temperatures below 800 K, the density fluctuation is dominated by compressibility; whereas, at a temperature of 1300 K, the contributions of compressibility and of mixing are about equal.

3) The time scale of the autocorrelation of Mach wave sound pressure increases linearly with axial distance downstream. This is consistent with a linear growth of the jet shear layer and a linear growth of the turbulent density fluctuation time scale. The Mach wave time scale varies inversely as the jet speed, indicating that the eddy length scales are independent of jet speed. The length scales of the eddies that contribute to Mach wave radiation grow linearly from a virtual origin for a jet of fixed Mach number.

4) The region of Mach wave emission increases from about 5 diam at 420 K to 12 diam at 1370 K. Over almost the entire extent of this region, the eddy convection velocity is constant, as indicated by the constancy of the Mach angle. The Mach angle ranged from 37 to 59 deg, becoming steeper as the temperature was increased and, hence, as the jet velocity was increased.

5) Mach waves contribute from 50% to almost 100% of the noise radiation depending on the location of their origin. The lower contribution that occurs at locations near the nozzle exit is due to radiation that appears to be centered in the transonic portion of the jet.

Acknowledgment

This paper represents one phase of research performed by the Jet Propulsion Laboratory, California Institute of Technology, sponsored by the National Aeronautics and Space Administration, Contract NAS7-100. The authors wish to express their sincere gratitude to S.B. Loewen for his significant contribution to the analysis of the data. In addition, the assistance of B. Dutt in conducting the experiments, F.H. Slover, W. Bixler, and D. Feller in fabricating, assembling, and testing, and S.J. Kikkert in data processing are greatly appreciated.

References

[1] Ffowcs-Williams, J.E. and Maidanik, G., "The Mach Wave Field Radiated by Supersonic Turbulent Shear Flows," *Journal of Fluid Mechanics*, Vol. 21, April 1965, pp. 641-657.

[2] Parthasarathy, S.P., Massier, P.F., Cuffel, R.F., and Radbill, Jr.,J.R., "Density Fluctuations and Radiated Noise for a High-Temperature Supersonic Jet." AIAA *Progress in Astronautics and Aeronautics—Aeroacoustics: Jet Noise, Combustion and Core Engine Noise,* Vol. 43, edited by Schwartz, Nagamatsu, and Strahle, New York, 1976, pp. 283-306.